B. M. Masini and A. Conti, "Adaptive TORC detection for MC-CDMA wireless systems," in IEEE Transactions on Communications, vol. 57, no. 11, pp. 3460-3471, Nov. 2009.
doi: 10.1109/TCOMM.2009.11.060439

Adaptive TORC Detection for MC-CDMA Wireless Systems

Barbara M. Masini, *Member, IEEE,* Andrea Conti, *Member, IEEE*

***Abstract*—Multi carrier code-division multiple access (MC-CDMA) is considered for beyond third generation wireless systems for its effectiveness in combating both multipath fading and interference still maintaining high data rate. This paper investigates MC-CDMA systems adopting an adaptive detection technique based on threshold orthogonality restoring combining (TORC). The mathematical framework here developed allows the evaluation of both the bit error probability and the bit error outage in downlink with perfect and imperfect channel state information and the derivation of the TORC threshold that optimizes the performance. The optimal threshold is analytically derived as a function of the number of subcarriers, the number of active users, and the mean signal-to-noise ratio. This enables an adaptive variation of the threshold following slow processes fluctuations. Numerical results show very good performance of TORC comparing with other combining techniques and demonstrate that the optimal threshold changes considering perfect and imperfect channel estimation. Results are shown both in uncorrelated Rayleigh fading as well as in time and frequency correlated fading channels.**

***Index Terms*—MC-CDMA, TORC detector, performance evaluation, fading channels, adaptive system.**

I. Introduction

Multi-carrier code division multiple access (MC-CDMA) technique is gaining interest for beyond third generation (B3G) mobile radio systems due to its efficiency in supporting high data rate mobile communication against both frequency selective fading and multi-user interference [1]–[3]. The suitability of MC-CDMA as multiple-access scheme derives from the combination of orthogonal frequency-division multiplexing (OFDM) and spreading. In this work we consider the system architecture presented in [2] and [4], where the spreading is performed in the frequency-domain and Walsh-Hadamard (W-H) codes are used with spreading factor equal to the number of subcarriers. The transmitter and receiver block schemes are depicted in Fig. 1.[1]

The main impairment of this multiplexing technique is represented by the multiple-access interference (MAI), which occurs in the presence of multipath fading propagation due to loss of orthogonality among the received spreading codes in spite of the use of W-H codes. Typically, the MAI mitigation is accomplished at the receiver using single-user or multiuser detection schemes, thus, the choice of the combining technique becomes critical and drastically affects the system performance. Several combining techniques with different complexities have been studied in the literature (see, e.g., [5]–[7]). In this paper, we address low complexity schemes such as linear combining, since in the downlink the detection is performed at the user terminal and we aim at proposing a simple adaptive combining technique.

Within the family of linear combining techniques, several schemes based on channel state information (CSI) are known in the literature (see, e.g., [8]–[10]), for which signals coming from different subcarriers are weighted by suitable coefficients g_m (m being the subcarriers index). The equal gain combining (EGC) technique consists in equally weighting each subchannel contribution and compensating only the phases with $g_m = h_m^*/|h_m|$, where h_m is the mth channel coefficient (notation * stands for complex conjugation). If the system is noise-limited, (i.e., the number of active users is negligible with respect to the number of subcarriers), maximal ratio combining (MRC), for which $g_m = h_m^*$, represents the best choice. On the other hand, this choice totally destroys the orthogonality between the codes in case of multiple users. For this reason, when the system is interference-limited, a good choice is given by restoring the orthogonality between the sequences as with the orthogonality restoring combining (ORC) technique, for which $g_m = h_m^*/|h_m|^2$. This implies a total cancellation of the multiuser interference but emphasizes the noise. This is corrected with threshold ORC (TORC), where a threshold is introduced to cancel the contributions of those subchannels highly corrupted by the noise, allowing good performance despite the low complexity (see [11]–[13]). Indeed, while EGC is desirable for its simplicity and MRC for its noise counteracting capability, neither of these techniques directly address the interference and the exploitation of the spreading codes. B3G communication systems intend to multiplex as many users as possible sharing the same resources, they are typically interference-limited; this is the reason why TORC is assuming an increasing interest. Since the orthogonality of the users is encoded in the phase of each subcarriers, TORC is mainly beneficial in the downlink where phase distortion may be more easily corrected rather than in the uplink [2].

Earlier works investigated the performance of MC-CDMA systems varying the detector; some of these involve TORC technique: in [4] and [13] the performance was studied by simulation or through semi-analytical models. In particular, the bit error probability (BEP) was approximated as the sum of the binomial distribution of the number of subcarriers

B. Masini {barbara.masini@unibo.it} is with WiLAB, IEIIT/CNR at the University of Bologna, Italy. A. Conti {a.conti@ieee.org} is with ENDIF, WiLAB, CNIT, University of Ferrara, Italy.

Manuscripted received July 28, 2006; revised February 13, 2008, and December 19, 2008; and accepted April 20, 2009. The editor coordinating the review of this paper and approving it for publication is G.E. Corazza.

This work has been inspired and supported in part by the FP7 European Network of Excellence NEWCom++.

Digital Object Identifier 10.1109/TCOMM.2009.XX.XXXXXX

[1]Note that these schemes are useful for the analysis, although typical implementation uses inverse and direct fast Fourier transform.

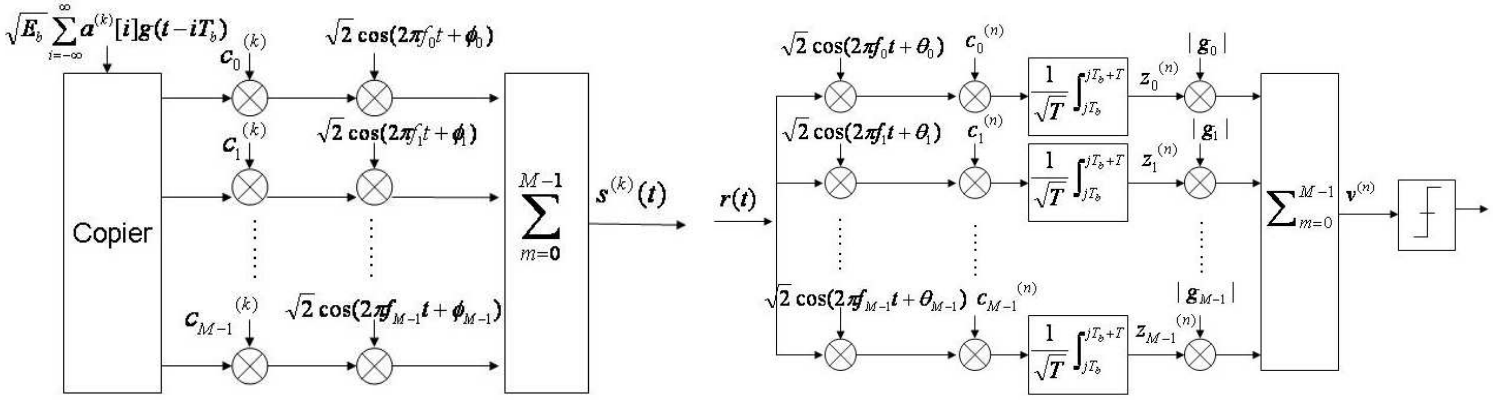

(a) Transmitter (b) Receiver

Fig. 1. Transmitter and receiver block schemes.

above the threshold, resulting in a cumbersome expression to be computed in closed form or implemented in upper layer simulators. In [12] the bit error rate (BER) was obtained by simulation. In [11] and [14] an analytical framework was proposed to derive the downlink BEP with TORC detector for synchronous users: in particular, in [11] decision-directed MC-CDMA detectors with and without explicit channel estimation are investigated; they also compared the decision-directed and pilot-aided approaches and explored the trade-off between channel estimation overhead and performance to verify how the channel estimation process affects the performance of MC-CDMA detectors with Kalman filter to track the channel.

In this paper, we mathematically derive a simple BEP approximation for downlink frequency selective fading channels adopting a TORC detector with both perfect and imperfect CSI. In addition to the BEP, our framework enables the investigation of the bit error outage (BEO), that is the BEP-based outage probability and represents a significant performance figure when small-scale fading is superimposed to large-scale fading [15]. We also analytically evaluate the optimal threshold and its relation with slow varying processes, such as the number of active users, the number of subcarriers, and the mean signal-to-noise ratio (SNR) averaged over small-scale fading. Imperfect CSI is also considered to analyze how the optimum threshold changes with respect to the case of perfect estimation. Note that, the number of active users, the number of subcarriers, and the mean SNR represent slow varying processes with respect to the variations in the performance perceived by the user, allowing an optimized and adaptive use of the threshold that can be changed tracking slow processes variation (for a discussion on slow and fast processes affecting the performance of adaptive and non-adaptive wireless communications see, e.g., [16], [17]). It will be shown that the proposed adaptive TORC, significantly improves the performance with respect to others linear combining techniques. Analytical results will be confirmed by simulations.

The rest of the paper is organized as follows: system model and methodology are described in Sec. II, the decision variable is given in Sec. III, and the BEP in Sec. IV. The optimal threshold is evaluated in Sec. V and the BEO in Sec. VI. Finally, numerical results and our conclusions are given in Sec. VII and Sec. VIII, respectively.

II. System Model and Methodology

In the considered MC-CDMA architecture, each data-symbol is copied over all subcarriers, and multiplied by the chip assigned to each particular subcarrier. We consider W-H orthogonal codes and binary phase shift keying (BPSK) modulation. Hence, the signal transmitted to the kth user can be written as (see Figg. 1(a)):

$$s^{(k)}(t) = \sqrt{\frac{2E_\mathrm{b}}{M}} \sum_{i=-\infty}^{+\infty} \sum_{m=0}^{M-1} c_m^{(k)} a^{(k)}[i] g(t - iT_\mathrm{b}) \times \cos(2\pi f_m t + \phi_m), \quad (1)$$

where E_b is the energy per bit, M is the number of subcarriers, m is the subcarrier index, c_m is the mth chip (taking values ± 1), $a^{(k)}[i]$ is the data-symbol transmitted during the symbol-time i, $g(t)$ is the pulse with rectangular waveform, duration $[0, T]$, and unitary energy, T_b is the bit-time, f_m is the mth subcarrier-frequency (with $\Delta f\, T$ and $f_0\, T$ integers to have orthogonality in frequency), and ϕ_m is the random phase uniformly distributed within $[-\pi, \pi)$. In particular, $T_\mathrm{b} = T + T_\mathrm{g}$ is the total OFDM symbol duration, increased with respect to T by a time-guard T_g (usually inserted between consecutive symbols to eliminate the residual inter symbol interference, ISI, due to the channel delay spread).

We assume a frequency-domain channel model in which the transfer function is considered constant in the bandwidth of each subcarrier and is given by:

$$h_m = \alpha_m e^{j\psi_m}, \quad (2)$$

where α_m and ψ_m are the mth amplitude and phase coefficients, respectively. Each h_m is assumed independent identically distributed (i.i.d.) complex zero-mean Gaussian random variable (RV) with variance per dimension σ_h^2, equal to $1/2$ so that $\mathbb{E}\left\{\alpha_m^2\right\} = 1$, for all m.[2]

[2] $\mathbb{E}\{\cdot\}$ denotes the statistical expectation, here with respect to realizations of α_m.

Assuming the coherence bandwidth smaller than the distance between two adjacent subcarriers (owing, for instance, to frequency interleaving), each α_m and ψ_m are considered independent; we assume that each subcarrier experiences flat fading. This represents a realistic case when the subcarriers are sufficiently spaced in frequency or when only a subset of the amount of subcarriers is used for the transmission of a symbol. Starting from these common assumptions, we analytically evaluate the performance in terms of BEP and we carefully investigate the performance dependencies on system parameters, then also allowing comparison with previous results appeared in the literature [3], [18], [19].

In the downlink, the system is assumed synchronous and the signal components associated to different users experiment the same fading. Furthermore, since the orthogonality of the users is encoded in the phase of the subcarriers, the TORC technique is primarily beneficial in the downlink where phase distortion for all users can be more easily corrected [2].[3] Hence, the received signal can be written as:

$$r(t) = \sqrt{\frac{2E_\mathrm{b}}{M}} \sum_{k=0}^{N_\mathrm{u}-1} \sum_{i=-\infty}^{+\infty} \sum_{m=0}^{M-1} \alpha_m c_m^{(n)} a^{(k)}[i] \tilde{g}(t - iT_\mathrm{b}) \times \cos(2\pi f_m t + \overbrace{\phi_m + \psi_m}^{\vartheta_m}) + n(t), \quad (3)$$

where summations are on users, symbols, and subcarriers, respectively, $\tilde{g}(t)$ is the response of the channel to the pulse $g(t)$ with unitary energy and duration $\tilde{T} \triangleq T + T_\mathrm{d}$, being T_d the pulse enlargement due to the overall distortion of the channel, $n(t)$ is the additive white Gaussian noise with two-side power spectral density $N_0/2$, and $\vartheta_m \triangleq \phi_m + \psi_m$ uniformly distributed in $[-\pi, \pi)$.

To analyze the performance with imperfect CSI, we assume a channel estimation error [20] on each subcarrier, e_m, complex Gaussian distributed with zero-mean and variance $2\sigma_\mathrm{e}^2$, thus $e_m \sim \mathcal{CN}(0, 2\sigma_\mathrm{e}^2)$, and we define the normalized channel estimation error variance as $\varepsilon \triangleq \sigma_\mathrm{e}^2/\sigma_\mathrm{h}^2$. The mth estimated complex channel coefficient is given by:

$$\hat{h}_m = h_m + e_m \,, \quad (4)$$

where, $\hat{h}_m = \hat{\alpha}_m e^{j\hat{\psi}_m}$.

By observing the receiver structure depicted in Fig. 1(b) and focusing on the lth subcarrier for the nth user (being in the downlink, perfect synchronization and phase tracking are assumed), the correlation output at the jth instant is given by:

$$z_l^{(n)}[j] = \frac{1}{\sqrt{T}} \int_{jT_\mathrm{b}}^{jT_\mathrm{b}+T} r(t)\; c_l^{(n)} \sqrt{2} \cos(2\pi f_l t + \hat{\vartheta}_l) dt \,. \quad (5)$$

Hence, substituting (3) in (5), the term $z_l^{(n)}[j]$ results as in (6), where:

$$w_{m,l}[j] = \begin{cases} \cos(\vartheta_l - \hat{\vartheta}_l) & m = l \\ 0 & m \neq l \,. \end{cases}$$

Since ISI is avoided, we will remove the time-index j in the following. After some manipulation we can write:

$$z_l^{(n)} = \sqrt{\frac{E_\mathrm{b}\delta_\mathrm{d}}{M}} \alpha_l \cos(\vartheta_l - \hat{\vartheta}_l) a^{(n)} + \sqrt{\frac{E_\mathrm{b}\delta_\mathrm{d}}{M}} c_l^{(n)} \alpha_l \cos(\vartheta_l - \hat{\vartheta}_l) \sum_{k=0, k\neq n}^{N_\mathrm{u}-1} c_l^{(k)} a^{(k)} + n_l \,, \quad (7)$$

where $\delta_\mathrm{d} \triangleq 1/(1 + T_\mathrm{d}/T)$ represents the loss of energy caused by the time-spreading, T_d, of the received pulse.

From the received signal expression before the combiner, we can now proceed to evaluate the performance in terms of BEP and BEO. The BEP averaged over small-scale fading is a common performance figure for applications in which the user's perceived quality of service (QoS) is related to the error rate observed in a time interval of several symbol times (see e.g., [17]). Thus, the variability of processes affecting the useful signal during this interval has to be carefully taken into account (e.g., the mean SNR, $\overline{\gamma}$, also varies due to the shadowing, but slowly with respect to the interval considered for the BEP evolution). For this reason, the BEO, that is the probability that the BEP exceeds a maximum tolerable level, is also an appropriate figure of merit for digital communication systems where small-scale fading is superimposed on large-scale fading, such as shadowing [15].

III. Decision Variable

The decision variable, $v^{(n)}$, is obtained by a linear combination of the weighted signals from each subcarrier as follows:

$$v^{(n)} = \sum_{l=0}^{M-1} |g_l| z_l^{(n)} \,. \quad (8)$$

The TORC detector consists in choosing the complex weight referring to the lth subcarrier as:

$$|g_l| = u(|\hat{h}_l| - \rho_\mathrm{TH})/|\hat{h}_l| = \hat{\alpha}_l^{-1} u(\hat{\alpha}_l - \rho_\mathrm{TH}) \,. \quad (9)$$

[3]Note that, in the downlink, power efficient mobile receivers with low complexity are required, whereas for the uplink, a high complexity multiuser detector can be used to cope with the presence of several users.

$$z_l^{(n)}[j] = 2\sqrt{\frac{E_\mathrm{b}}{MT}} \sum_{i=-\infty}^{+\infty} \int_{jT_\mathrm{b}}^{jT_\mathrm{b}+T} \sum_{k=0}^{N_\mathrm{u}-1} \sum_{m=0}^{M-1} \alpha_m c_m^{(k)} c_l^{(n)} a^{(k)}[i] \tilde{g}(t - iT_\mathrm{b}) \cos(2\pi f_m t + \vartheta_m) \cos(2\pi f_l t + \hat{\vartheta}_l) dt \quad (6)$$

$$+ \overbrace{\int_{jT_\mathrm{b}}^{jT_\mathrm{b}+T} \sqrt{2} \frac{c_l^{(n)}}{\sqrt{T}} n(t) \cos(2\pi f_l t + \hat{\vartheta}_l) dt}^{n_l[j]} = \sqrt{\frac{E_\mathrm{b}}{M}} \frac{T}{\tilde{T}} \sum_{k=0}^{N_\mathrm{u}-1} \sum_{m=0}^{M-1} \overbrace{\frac{1}{T} \int_{jT_\mathrm{b}}^{jT_\mathrm{b}+T} 2\cos(2\pi f_m t + \vartheta_m) \cos(2\pi f_l t + \hat{\vartheta}_l) dt}^{w_{m,l}[j]}$$

$$\times\; \alpha_m c_m^{(k)} c_l^{(n)} a^{(k)}[j] + n_l[j] = \sqrt{\frac{E_\mathrm{b}}{M}} \frac{T}{\tilde{T}} \left\{ \sum_{k=0}^{N_\mathrm{u}-1} \alpha_l c_l^{(k)} c_l^{(n)} a^{(k)}[j] u_{l,l}[j] + \sum_{m=0, m\neq l}^{M-1} \sum_{k=0}^{N_\mathrm{u}-1} \alpha_m c_m^{(k)} c_l^{(n)} a^{(k)}[j] u_{m,l}[j] \right\} + n_l[j]$$

where $u(\cdot)$ is the unitary-step function and ρ_{TH} is the positive threshold introduced to cancel the contributions of those sub-channels highly corrupted by the noise. Hence, by substituting (7) and (9) in (8) we can write:

$$v^{(n)} = \overbrace{\sqrt{\frac{E_{\text{b}}\delta_{\text{d}}}{M}} \sum_{l=0}^{M-1} u(\hat{\alpha}_l - \rho_{\text{TH}})\alpha_l \hat{\alpha}_l^{-1} \cos(\vartheta_l - \hat{\vartheta}_l)\, a^{(n)}}^{U} + \overbrace{\sqrt{\frac{E_{\text{b}}\delta_{\text{d}}}{M}} \sum_{l=0}^{M-1} c_l^{(n)} u(\hat{\alpha}_l - \rho_{\text{TH}})\alpha_l \hat{\alpha}_l^{-1} \cos(\vartheta_l - \hat{\vartheta}_l)}^{I} \times \overbrace{\sum_{k=0,k\neq n}^{N_{\text{u}}-1} c_l^{(k)} a^{(k)}}^{\text{in } I} + \overbrace{\sum_{l=0}^{M-1} n_l \hat{\alpha}_l^{-1} u(\hat{\alpha}_l - \rho_{\text{TH}})}^{N}, \quad (10)$$

where the three terms U, I, and N represent the useful, interfering, and noise term, respectively.
By defining

$$\Theta_l(\rho_{\text{TH}}) \triangleq u(\hat{\alpha}_l - \rho_{\text{TH}})\alpha_l \hat{\alpha}_l^{-1} \cos(\vartheta_l - \hat{\vartheta}_l), \quad (11)$$

we can write (10) as in the following:

$$v^{(n)} = U \cdot a^{(n)} + I + N, \quad (12)$$

where

$$U = \sqrt{\frac{E_{\text{b}}\delta_{\text{d}}}{M}} \sum_{l=0}^{M-1} \Theta_l(\rho_{\text{TH}}) \quad (13)$$

$$I = \sqrt{\frac{E_{\text{b}}\delta_{\text{d}}}{M}} \sum_{l=0}^{M-1} c_l^{(n)} \Theta_l(\rho_{\text{TH}}) \sum_{k=0,k\neq n}^{N_{\text{u}}-1} c_l^{(k)} a^{(k)} \quad (14)$$

$$N = \sum_{l=0}^{M-1} n_l \hat{\alpha}_l^{-1} u(\hat{\alpha}_l - \rho_{\text{TH}}). \quad (15)$$

Hence, in order to derive the BEP, we need the statistic distribution of $v^{(n)}$ that can be obtained by studying the statistics of U, I, and N. By considering that actual and future multi carrier systems generally have a high number of subcarriers (e.g., 2k or 8k for digital video broadcasting), we will adopt the central limit theorem (CLT) and the law of large number (LLN) to approximate the BEP (the goodness of the approximation will also be verified by simulation).

A. Useful Term

By applying the CLT,[4] the useful term U in (10) results distributed as[5]

$$U \sim \mathcal{N}\left(\mu_U, \sigma_U^2\right). \quad (16)$$

The mean and variance of U are respectively given by $\mu_U = \sqrt{E_{\text{b}}\delta_{\text{d}}M}\, \mathbb{E}\{\Theta(\rho_{\text{TH}})\}$ and $\sigma_U^2 = E_{\text{b}}\delta_{\text{d}}[\mathbb{E}\left\{\Theta^2(\rho_{\text{TH}})\right\} - (\mathbb{E}\{\Theta(\rho_{\text{TH}})\})^2]$.[6]

[4]CLT has been applied to analyze MC-CDMA systems also, e.g., in [2] and [4].

[5]Notation $\mathcal{N}(\mu, \sigma^2)$ stands for Gaussian distribution with mean μ and variance σ^2.

[6]Note that $\mathbb{E}\{\Theta(\rho_{\text{TH}})\}$ is independent on index l.

B. Interference Term

By partitioning orthogonal codes as in [4], after some mathematical manipulation we derive the interference as:

$$I = \sqrt{\frac{E_{\text{b}}\delta_{\text{d}}}{M}} \sum_{k=0,k\neq n}^{N_{\text{u}}-1} a^{(k)} \times \left[\overbrace{\sum_{h=1}^{\frac{M}{2}} \Theta_{x_h}(\rho_{\text{TH}})}^{\Lambda_1} - \overbrace{\sum_{h=1}^{\frac{M}{2}} \Theta_{y_h}(\rho_{\text{TH}})}^{\Lambda_2} \right], \quad (17)$$

where indexes x_h and y_h define the following partitions:

$$c_{x_h}^{(n)} c_{x_h}^{(k)} = 1$$
$$c_{y_h}^{(n)} c_{y_h}^{(k)} = -1$$
$$\{x_h\} \cup \{y_h\} = 0, 1, ..., M-1.$$

For large values of M, we apply the CLT to terms Λ_1 and Λ_2 in (17), consequently we obtain:

$$\Lambda_1, \Lambda_2 \sim \mathcal{N}\left(\sqrt{\frac{M}{2}}\mathbb{E}\{\Theta(\rho_{\text{TH}})\}, \frac{M}{2}\zeta_\alpha(\Theta)\right), \quad (18)$$

where $\zeta_\alpha(\Theta) = \mathbb{E}\left\{\Theta^2(\rho_{\text{TH}})\right\} - \mathbb{E}\{\Theta(\rho_{\text{TH}})\}^2$. Hence, by exploiting the symmetry of the Gaussian probability density function (p.d.f.) and the property of the sum of uncorrelated Gaussian RVs, we have:

$$a^{(k)}(\Lambda_1 - \Lambda_2) \sim \mathcal{N}(0, M\zeta_\alpha(\Theta)).$$

Then, the general interference term results distributed as:

$$I \sim \mathcal{N}\left(0, \sigma_{\text{I}}^2\right), \quad (19)$$

where $\sigma_{\text{I}}^2 = E_{\text{b}}\delta_{\text{d}}(N_{\text{u}} - 1)\left[\mathbb{E}\left\{\Theta^2(\rho_{\text{TH}})\right\} - \mathbb{E}\{\Theta(\rho_{\text{TH}})\}^2\right]$.

C. Noise Term

Since terms $\hat{\alpha}_l$ and n_l in N are independent and n_l has mean equal to zero, the total noise term consists in a sum of i.i.d. zero mean RVs with variance $(N_0/2)\,\mathbb{E}\left\{(\hat{\alpha}^{-1}u(\hat{\alpha} - \rho_{\text{TH}}))^2\right\}$. By applying the CLT, the noise term results distributed as:

$$N \sim \mathcal{N}\left(0, \sigma_{\text{N}}^2\right), \quad (20)$$

with $\sigma_{\text{N}}^2 = M\ (N_0/2)\ \mathbb{E}\left\{(\hat{\alpha}^{-1}u(\hat{\alpha} - \rho_{\text{TH}}))^2\right\}$.

The expressions of $\mathbb{E}\{\Theta(\rho_{\text{TH}})\}$, $\mathbb{E}\left\{\hat{\alpha}^{-2}u^2(\hat{\alpha} - \rho_{\text{TH}})\right\}$, and $\mathbb{E}\left\{\Theta^2(\rho_{\text{TH}})\right\}$ are derived in the Appendix, and result in:

$$\mathbb{E}\{\Theta(\rho_{\text{TH}})\} = e^{-\frac{\rho_{\text{TH}}^2}{2\sigma_{\text{h}}^2(1+\varepsilon)}} - \frac{2\varepsilon\ e^{-\frac{\rho_{\text{TH}}^2(1+3\varepsilon/4)}{2\sigma_{\text{h}}^2(1+\varepsilon)}}}{(1-\varepsilon^2)(4+3\varepsilon)}$$

$$\mathbb{E}\left\{\hat{\alpha}^{-2}u^2(\hat{\alpha} - \rho_{\text{TH}})\right\} = \frac{1}{2\sigma_{\text{h}}^2(1+\varepsilon)}\Gamma\left[0, \frac{\rho_{\text{TH}}^2}{2\sigma_{\text{h}}^2(1+\varepsilon)}\right]$$

$$\mathbb{E}\left\{\Theta^2(\rho_{\text{TH}})\right\} = e^{-\frac{\rho_{\text{TH}}^2}{2\sigma_{\text{h}}^2(1+\varepsilon)}} - \frac{4\varepsilon\ e^{-\frac{\rho_{\text{TH}}^2(1+3\varepsilon/4)}{2\sigma_{\text{h}}^2(1+\varepsilon)}}}{(1-\varepsilon^2)(4+3\varepsilon)} + C(B_1 + B_2 + B_3 + B_4), \quad (21)$$

where the expressions of C, B_1, B_2, B_3 and B_4 are given in the Appendix.

D. Independence between terms

Since $a^{(k)}$ is zero mean and statistically independent on α_l, $(\Lambda_1 - \Lambda_2)$, and n_l, we can write that $\mathbb{E}\{IN\} = \mathbb{E}\{IU\} = 0$. Since n_l and α_l are statistically independent, then $\mathbb{E}\{NU\} = 0$. Moreover I, N, and U are uncorrelated Gaussian RVs, thus also statistically independent.

IV. Bit Error Probability Evaluation

From the statistical distribution of the terms I and N, the total disturbance (interference plus noise) results to be Gaussian distributed as:

$$I + N \sim \mathcal{N}\left(0, \sigma_{\mathrm{I}}^2 + \sigma_{\mathrm{N}}^2\right) . \tag{22}$$

This enables us to derive the BEP approximation as a function of the mean SNR $\overline{\gamma}$, the TORC threshold ρ_{TH}, the number of subcarriers M, the number of active users N_{u}, and the channel estimation error related to ε.
The BEP conditioned to the RV U is given by:

$$P_{\mathrm{b}}|_U = \frac{1}{2}\mathrm{erfc}\left\{\frac{U}{\sqrt{2(\sigma_{\mathrm{I}}^2 + \sigma_{\mathrm{N}}^2)}}\right\} , \tag{23}$$

where erfc is the complementary error function. By applying the LLN, that is by approximating $\sum_{l=0}^{M-1}\Theta_l(\rho_{\mathrm{TH}})$ with $M\mathbb{E}\{\Theta(\rho_{\mathrm{TH}})\}$, we derive the unconditioned BEP as:

$$P_{\mathrm{b}} \simeq \frac{1}{2}\mathrm{erfc}\left(\frac{\sqrt{E_{\mathrm{b}}\delta_{\mathrm{d}}M}\ \mathbb{E}\{\Theta(\rho_{\mathrm{TH}})\}}{\sqrt{2(\sigma_{\mathrm{N}}^2 + \sigma_{\mathrm{I}}^2)}}\right) . \tag{24}$$

From the expressions of σ_{I}^2, σ_{N}^2, and $\mathbb{E}\{\Theta(\rho_{\mathrm{TH}})\}$ derived above, the BEP can be written as a function of the signal-to-interference-plus-noise ratio (SINR) as in the following:

$$P_{\mathrm{b}}\left(\overline{\zeta}\right) \simeq \frac{1}{2}\mathrm{erfc}\left(\sqrt{\overline{\zeta}}\right) , \tag{25}$$

where $\overline{\zeta}$ is the mean SINR averaged over small-scale fading and is given by:

$$\overline{\zeta} = \frac{\overline{\gamma}\ e^{-\frac{\rho_{\mathrm{TH}}^2}{\sigma_{\mathrm{h}}^2(1+\varepsilon)}} f_1(\varepsilon,\rho_{TH})}{\frac{1}{(1+\varepsilon)}\Gamma[0,\frac{\rho_{\mathrm{TH}}^2}{2\sigma_{\mathrm{h}}^2(1+\varepsilon)}] + 2\frac{N_{\mathrm{u}}-1}{M} f_2(\varepsilon,\rho_{TH})\overline{\gamma}} . \tag{26}$$

In (26), $\overline{\gamma} \triangleq E_{\mathrm{b}}\delta_{\mathrm{d}}2\sigma_{\mathrm{h}}^2/N_0$ is the mean SNR averaged over small-scale fading and

$$\begin{aligned} f_1(\varepsilon,\rho_{TH}) &= \left(1 - \frac{2\varepsilon}{(1-\varepsilon^2)(4+3\varepsilon)} e^{-\frac{\rho_{\mathrm{TH}}^2}{8\sigma_{\mathrm{h}}^2(1+\varepsilon)}3\varepsilon}\right)^2 \\ f_2(\varepsilon,\rho_{TH}) &= e^{-\frac{\rho_{\mathrm{TH}}^2}{2\sigma_{\mathrm{h}}^2(1+\varepsilon)}}\left[1 - \frac{4\varepsilon e^{-\frac{\rho_{\mathrm{TH}}^2}{8\sigma_{\mathrm{h}}^2(1+\varepsilon)}3\varepsilon}}{(1-\varepsilon^2)(4+3\varepsilon)}\right] \\ &\quad + e^{\frac{\rho_{\mathrm{TH}}^2}{2\sigma_{\mathrm{h}}^2(1+\varepsilon)}} C(B_1+B_2+B_3+B_4) \\ &\quad - e^{-\frac{\rho_{\mathrm{TH}}^2}{\sigma_{\mathrm{h}}^2(1+\varepsilon)}}\left[1 - \frac{2\varepsilon e^{\frac{-\rho_{\mathrm{TH}}^2}{8\sigma_{\mathrm{h}}^2(1+\varepsilon)}3\varepsilon}}{(4+3\varepsilon)(1-\varepsilon^2)}\right]^2 . \end{aligned}$$

In case of perfect CSI, (26) reduces to:

$$\overline{\zeta} = \frac{\overline{\gamma}\ e^{-\frac{\rho_{\mathrm{TH}}^2}{\sigma_{\mathrm{h}}^2}}}{\Gamma[0,\frac{\rho_{\mathrm{TH}}^2}{2\sigma_{\mathrm{h}}^2}] + 2\frac{N_{\mathrm{u}}-1}{M}\left(e^{-\frac{\rho^2}{2\sigma_{\mathrm{h}}^2}} - e^{-\frac{\rho^2}{\sigma_{\mathrm{h}}^2}}\right)\overline{\gamma}} . \tag{27}$$

Remark: Note that the main objective of this work is not only to assess a tight approximation for the BEP, but mostly to derive the value of the TORC threshold, ρ_{TH}, which minimizes the BEP depending on the other system parameters. From this point of view, we will show a good agreement between simulative and analytical results in Sec. VII.

V. TORC Threshold Optimization

We aim at finding the optimum value of the threshold, $\rho_{\mathrm{TH}}^{(\mathrm{opt})}$, defined as the value that minimizes the BEP (hence that maximizes the SINR since the BEP in (25) is monotonically decreasing with the SINR):

$$\rho_{\mathrm{TH}}^{(\mathrm{opt})} = \arg\min_{\rho_{\mathrm{TH}}}\{P_{\mathrm{b}}\} = \arg\max_{\rho_{\mathrm{TH}}}\{\overline{\zeta}\} . \tag{28}$$

A. Optimal TORC with Non-Ideal Channel Estimation

By forcing to zero the derivative of the argument in (28) and remembering that $\overline{\gamma} > 0$, $\Gamma[0, 1/[2\sigma_{\mathrm{h}}^2(1+\varepsilon)]] > 0$, and $\rho_{\mathrm{TH}} \geq 0$, we obtain:

$$\begin{aligned} &\left(-\frac{2\rho_{\mathrm{TH}}}{\sigma_{\mathrm{h}}^2(1+\varepsilon)} f_1(\varepsilon,\rho_{\mathrm{TH}}) + f_1'(\varepsilon,\rho_{\mathrm{TH}})\right) \\ &\times \left(\frac{\Gamma\left[0,\frac{\rho_{\mathrm{TH}}^2}{2\sigma_{\mathrm{h}}^2(1+\varepsilon)}\right]}{(1+\varepsilon)} + 2\frac{N_{\mathrm{u}}-1}{M} f_2(\varepsilon,\rho_{TH})\overline{\gamma}\right) \\ &= f_1(\varepsilon,\rho_{\mathrm{TH}})\left[\frac{\Gamma'\left[0,\frac{\rho_{\mathrm{TH}}^2}{2\sigma_{\mathrm{h}}^2(1+\varepsilon)}\right]}{(1+\varepsilon)} + 2\frac{N_{\mathrm{u}}-1}{M} f_2'(\varepsilon,\rho_{TH})\overline{\gamma}\right] , \end{aligned} \tag{29}$$

where $f'(\cdot)$ stands for the first derivative of $f(\cdot)$ evaluated with respect to ρ_{TH}. Let us now define the system load as

$$\eta \triangleq \frac{N_{\mathrm{u}}-1}{M} , \tag{30}$$

and the parameter ξ as

$$\xi \triangleq 2\overline{\gamma}\eta . \tag{31}$$

Since

$$\Gamma'\left[0,\frac{\rho_{\mathrm{TH}}^2}{2\sigma_{\mathrm{h}}^2(1+\varepsilon)}\right] = -\frac{2}{\rho_{\mathrm{TH}}} e^{-\rho_{\mathrm{TH}}^2/(2(1+\varepsilon)\sigma_{\mathrm{h}}^2)} ,$$

the (29) becomes as in (32) (bottom of the next page), where

$$\begin{aligned} f_1'(\varepsilon,\rho_{\mathrm{TH}}) &= \frac{\rho_{\mathrm{TH}} 3\varepsilon^2}{\sigma_{\mathrm{h}}^2(1+\varepsilon)(1-\varepsilon^2)(4+3\varepsilon)} e^{-\frac{\rho_{\mathrm{TH}}^2}{8\sigma_{\mathrm{h}}^2}\frac{3\varepsilon}{(1+\varepsilon)}} \\ &\quad \times \left[1 - \frac{2\varepsilon}{(1-\varepsilon^2)(4+3\varepsilon)} e^{-\frac{\rho_{\mathrm{TH}}^2}{8\sigma_{\mathrm{h}}^2}\frac{(3\varepsilon)}{(1+\varepsilon)}}\right] \end{aligned} \tag{33}$$

and

$$f_2'(\varepsilon,\rho_{\text{TH}}) = \frac{\rho_{\text{TH}}}{\sigma_{\text{h}}^2(1+\varepsilon)} e^{-\frac{\rho_{\text{TH}}^2}{2\sigma_{\text{h}}^2}(1+\varepsilon)} \left[\frac{\varepsilon e^{-\frac{\rho_{\text{TH}}^2}{8\sigma_{\text{h}}^2(1+\varepsilon)}3\varepsilon}}{(1-\varepsilon^2)} - 1 \right]$$
$$+ \frac{\rho_{\text{TH}}}{\sigma_{\text{h}}^2(1+\varepsilon)} e^{\frac{\rho_{\text{TH}}^2}{2\sigma_{\text{h}}^2}(1+\varepsilon)} C\left(B_1+B_2+B_3+B_4\right)$$
$$+ \frac{2\rho_{\text{TH}}}{\sigma_{\text{h}}^2(1+\varepsilon)} e^{-\frac{\rho_{\text{TH}}^2}{\sigma_{\text{h}}^2}(1+\varepsilon)} \left(1 - \frac{2\varepsilon e^{-\frac{\rho_{\text{TH}}^2}{8\sigma_{\text{h}}^2(1+\varepsilon)}3\varepsilon}}{(1-\varepsilon^2)(4+3\varepsilon)} \right)^2$$
$$- \frac{\rho_{\text{TH}}}{\sigma_{\text{h}}^2(1+\varepsilon)} e^{-\frac{\rho_{\text{TH}}^2}{2\sigma_{\text{h}}^2}(1+\varepsilon)}$$
$$\times \left[\frac{3\varepsilon^2 e^{-\frac{\rho_{\text{TH}}^2}{8\sigma_{\text{h}}^2(1+\varepsilon)}3\varepsilon}}{(1-\varepsilon^2)(4+3\varepsilon)} \left(1 - \frac{2\varepsilon e^{-\frac{\rho_{\text{TH}}^2}{8\sigma_{\text{h}}^2(1+\varepsilon)}3\varepsilon}}{(1-\varepsilon^2)(4+3\varepsilon)} \right) \right]. \quad (34)$$

It is important to note that the parameter ξ quantifies how the system is noise-limited (low values) or interference-limited (high values) and represents the implicit solution for the problem of finding the optimum value of ρ_{TH} for all possible values of SNR, number of subcarriers, and number of active users with non-ideal channel estimation. Thus, for each combination of the system parameters, there is a value of ρ_{TH} that minimizes the BEP. In addition, it is important to observe that ρ_{TH} only depends, through ξ, on processes slowly varying with respect to the performance perceived by the users. Hence, we propose and investigate an adaptive TORC detection in which ρ_{TH} is slowly adapted to the optimum value for the current set of parameters $\overline{\gamma}$, M, and N_{u}, for a given ε.

B. Optimal TORC with Ideal Channel Estimation

In the case of ideal CSI ($e_m = 0$ in (4)), then $\hat{h}_m = h_m$ for all m. Hence, $\varepsilon = 0$ and (26) becomes

$$\overline{\zeta} = \frac{\overline{\gamma}\, e^{-\frac{\rho_{\text{TH}}^2}{\sigma_{\text{h}}^2}}}{2^{\frac{N_{\text{u}}-1}{M}} \left(e^{-\frac{\rho_{\text{TH}}^2}{2\sigma_{\text{h}}^2}} - e^{-\frac{\rho_{\text{TH}}^2}{\sigma_{\text{h}}^2}} \right) \overline{\gamma} + \Gamma\left[0, \frac{\rho_{\text{TH}}^2}{2\sigma_{\text{h}}^2}\right]}. \quad (35)$$

For what concern the minimization of the BEP, the solving equation giving the optimum ρ_{TH} results:

$$\xi = 2\left(\frac{\sigma_H^2}{\rho_{\text{TH}}^2} - e^{\frac{\rho_{\text{TH}}^2}{2\sigma_{\text{h}}^2}} \Gamma\left[0, \frac{\rho_{\text{TH}}^2}{2\sigma_{\text{h}}^2}\right] \right). \quad (36)$$

As can be observed, the expression of ξ as a function of ρ_{TH} given by (32) is rather complex with respect to (36), thus the evaluation of the optimum threshold is more complicated when errors on the channel estimation occur. However, as will be verified in Sec. VII-A, for several situation of interest, the optimum threshold is almost the same in both cases, with perfect and imperfect CSI. This means that a system designer can adopt the value of the threshold in perfect CSI conditions also in presence of channel estimation errors.

VI. Bit Error Outage

In digital wireless communications where small-scale fading is superimposed to large-scale fading (i.e., shadowing) [21], another important performance metric is given by the BEO, defined as the probability that the BEP exceeds a maximum tolerable level (i.e., the target BEP, $P_{\text{b}}^\star$) [15]:

$$P_{\text{o}} \triangleq \mathbb{P}\{P_{\text{b}} > P_{\text{b}}^\star\} = \mathbb{P}\{\overline{\gamma}_{\text{dB}} < \overline{\gamma}_{\text{dB}}^\star\}, \quad (37)$$

where $\overline{\gamma}_{\text{dB}} = 10\log_{10}\overline{\gamma}$, and $\overline{\gamma}_{\text{dB}}^\star$ is the SNR (in dB) giving the BEP equal to $P_{\text{b}}^\star$ (i.e., $P_{\text{b}}(\overline{\gamma}^\star) = P_{\text{b}}^\star$).

We consider the case of a shadowing environment in which $\overline{\gamma}$ is log-normal distributed with parameters μ_{dB} and σ_{dB}^2 (i.e., $\overline{\gamma}_{\text{dB}}$ is a Gaussian RV with mean μ_{dB} and variance σ_{dB}^2). Hence, the BEO results in

$$P_{\text{o}} = \frac{1}{2}\text{erfc}\left\{ \frac{\mu_{\text{dB}} - \overline{\gamma}_{dB}^\star}{\sqrt{2}\sigma_{\text{dB}}} \right\}. \quad (38)$$

By inverting (25), the target SINR giving a BEP equal to the target BEP $P_{\text{b}}^\star$ is

$$\overline{\zeta}^\star = \left(\text{erfc}^{-1}\{2P_{\text{b}}^\star\}\right)^2, \quad (39)$$

where erfc^{-1} is the inverse complementary error function. Hence, we derive the required SNR, $\overline{\gamma}^\star$, as a function of $\overline{\zeta}^\star$, ρ_{TH}, and η, as given by:

$$\overline{\gamma}^\star = \frac{\overline{\zeta}^\star \Gamma\left[0, \frac{\rho_{\text{TH}}^2}{2\sigma_{\text{h}}^2(1+\varepsilon)}\right]}{(1+\varepsilon)\left[f_1(\varepsilon,\rho_{TH}) e^{-\frac{\rho_{TH}}{\sigma_{\text{h}}^2(1+\varepsilon)}} - 2\eta\overline{\zeta}^\star f_2(\varepsilon,\rho_{TH}) \right]} \quad (40)$$

that, in case of perfect CSI reduces to:

$$\overline{\gamma}^\star = \frac{\overline{\zeta}^\star\ \Gamma\left[0, \frac{\rho_{\text{TH}}^2}{2\sigma_{\text{h}}^2}\right]}{e^{-\frac{\rho_{\text{TH}}^2}{\sigma_{\text{h}}^2}} - 2\eta\overline{\zeta}^\star \left(e^{-\frac{\rho_{\text{TH}}^2}{2\sigma_{\text{h}}^2}} - e^{-\frac{\rho_{\text{TH}}^2}{\sigma_{\text{h}}^2}} \right)}. \quad (41)$$

The equation (40) (or (41) with perfect CSI) enables the derivation of the optimal ρ_{TH} which minimizes the required SINR for a target $P_{\text{b}}^\star$ and a given system load η. In addition, given the target BEP and BEO, from (40) (or (41) with perfect CSI) and (38) we obtain the required value of μ_{dB} that is the median value of the SNR; this is useful for wireless digital communication systems design, since it is strictly related to the link budget when the path-loss law is known.

$$\xi = \frac{\frac{1}{1+\varepsilon}\left(\frac{2\rho_{\text{TH}}}{\sigma_{\text{h}}^2(1+\varepsilon)} f_1(\varepsilon,\rho_{\text{TH}})\Gamma[0, \frac{\rho_{\text{TH}}^2}{2\sigma_{\text{h}}^2(1+\varepsilon)}] - \frac{2f_1(\varepsilon,\rho_{\text{TH}})}{\rho_{\text{TH}}} e^{-\frac{\rho_{\text{TH}}^2}{2\sigma_{\text{h}}^2(1+\varepsilon)}} - f_1'(\varepsilon,\rho_{\text{TH}})\Gamma[0, \frac{\rho_{\text{TH}}^2}{2\sigma_{\text{h}}^2(1+\varepsilon)}] \right)}{f_1'(\varepsilon,\rho_{\text{TH}}) f_2(\varepsilon,\rho_{TH}) - f_1(\varepsilon,\rho_{\text{TH}}) f_2'(\varepsilon,\rho_{TH}) - \frac{2\rho_{\text{TH}}}{\sigma_{\text{h}}^2(1+\varepsilon)} f_1(\varepsilon,\rho_{\text{TH}}) f_2(\varepsilon,\rho_{TH})}, \quad (32)$$

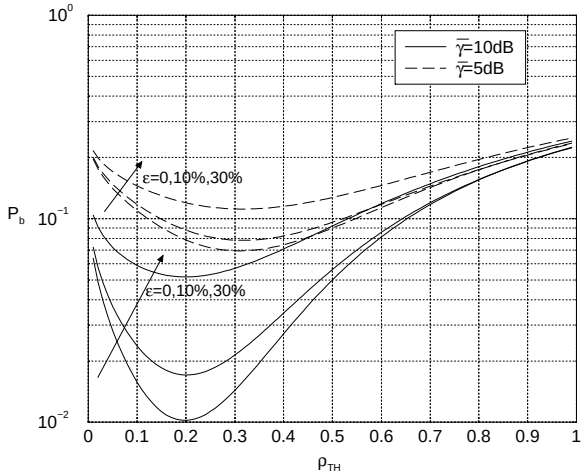

Fig. 2. BEP vs. ρ_{TH} varying the mean SNR $\overline{\gamma}$, and the variance of the channel estimation errors for $M = N_{\text{u}} = 1024$.

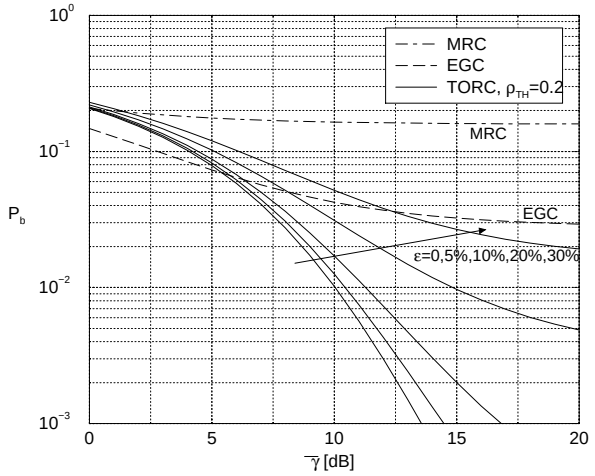

Fig. 3. BEP vs. $\overline{\gamma}$ in dB varying the variance of the channel estimation error for $M = N_{\text{u}} = 1024$ with $\rho_{\text{TH}} = 0.2$. A comparison with MRC and EGC techniques with perfect CSI is also reported.

By fixing the target performance in terms of $P_{\text{b}}^{\star}$, starting from (26) and remembering the expressions of η, we can derive the relation between η, $\overline{\gamma}^{\star}$, ρ_{TH}, and $\overline{\zeta}^{\star}$ as given by

$$\eta = \frac{\overline{\gamma}^{\star} f_1(\varepsilon, \rho_{TH}) e^{-\frac{\rho_{TH}}{\sigma}^2_{\text{h}}(1+\varepsilon)} - \frac{\overline{\zeta}^{\star}}{1+\varepsilon}\Gamma\left[0, \frac{\rho_{\text{TH}}^2}{2\sigma_{\text{h}}^2(1+\varepsilon)}\right]}{2\overline{\zeta}^{\star}\overline{\gamma}^{\star} f_2(\varepsilon, \rho_{TH})}, \quad (42)$$

that, in case of perfect CSI reduces to:

$$\eta = \frac{\overline{\gamma}^{\star}\ e^{-\frac{\rho^2}{\sigma_H^2}} - \overline{\zeta}^{\star}\ \Gamma[0, \frac{\rho^2}{2\sigma_{\text{h}}^2}]}{2\overline{\zeta}^{\star}\overline{\gamma}^{\star}\left(e^{-\frac{\rho^2}{2\sigma_{\text{h}}^2}} - e^{-\frac{\rho^2}{\sigma_{\text{h}}^2}}\right)}. \quad (43)$$

VII. Numerical Results

In this section, numerical results related to the BEP and the BEO for the downlink of MC-CDMA systems with optimized TORC detection are provided and compared with those of other combining techniques. Both ideal and non-ideal channel estimation are considered in uncorrelated Rayleigh fading as well as in time and frequency correlated channels.

A. Non-Ideal Channel Estimation

We now present analytical results in the presence of channel estimation error and we compare the BEP obtained with TORC detector with the BEP given by MRC and EGC.

In Fig. 2, the BEP given by (25) as a function of the TORC threshold ρ_{TH}, is presented when the system is fully loaded with $N_{\text{u}} = M = 1024$ as a function of the mean SNR $\overline{\gamma}$. The optimum value of ρ_{TH} minimizing the BEP can be observed. Moreover, the effect of channel estimation errors is shown and compared with the case of perfect CSI ($\varepsilon = 0$). In particular, a normalized variance of channel estimation errors, $\varepsilon = 0$, 10%, and 30% is considered. Note that ρ_{TH} strongly affects the BEP: in fact, focusing on the curves related to $\overline{\gamma} = 10$ dB and $\varepsilon = 10\%$, a $P_{\text{b}} \simeq 7.3 \cdot 10^{-2}$ is given by adopting a value of $\rho_{\text{TH}} = 0$ (ORC), while $P_{\text{b}} \simeq 1.7 \cdot 10^{-2}$ with $\rho_{\text{TH}} = 0.2$.
It is also important to observe that, in spite of the presence of channel estimation errors, the optimum value of the threshold minimizing the BEP does not significantly change with ε for a given value of mean SNR. Hence, the optimum value of ρ_{TH} for perfect CSI in (36) represents a good solution also in the case of channel estimation errors.

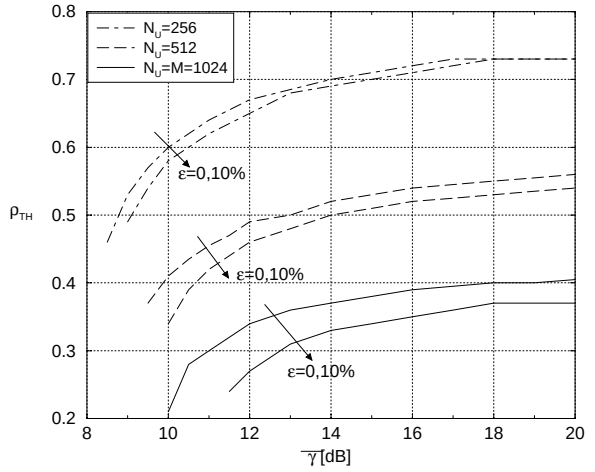

Fig. 4. Optimum value of ρ_{TH} vs. $\overline{\gamma}$ in dB giving $P_{\text{b}}^{\star} = 10^{-2}$ when varying the system load and the variance of the channel estimation error.

In Fig. 3, the BEP as a function of the mean SNR $\overline{\gamma}$, is shown when $\rho_{\text{TH}} = 0.2$ varying the normalized variance of the channel estimation errors ε. The system is assumed fully loaded with $N_{\text{u}} = M = 1024$. A comparison with MRC and EGC techniques (these with perfect CSI) is presented. As can be observed, TORC detection always outperforms MRC also when ε is not zero. On the other hand, EGC outperforms TORC detection for low values of mean SNR due to a sub-optimum value of the threshold. In fact, as we can see from Fig. 2, $\rho_{\text{TH}} = 0.2$ is optimum when $\overline{\gamma} = 10$ dB, but the optimum value changes with the mean SNR. However, as $\overline{\gamma}$ increases, TORC outperforms EGC.

In Fig. 4, the value of the threshold ρ_{TH} giving $P_{\text{b}} = P_{\text{b}}^{\star} = 10^{-2}$ (which is a typical value for uncoded systems) is plotted as a function of the mean SNR $\overline{\gamma}$ for fully loaded ($N_{\text{u}} = M = 1024$), half loaded ($N_{\text{u}} = 512$) and a quarter loaded ($N_{\text{u}} =$

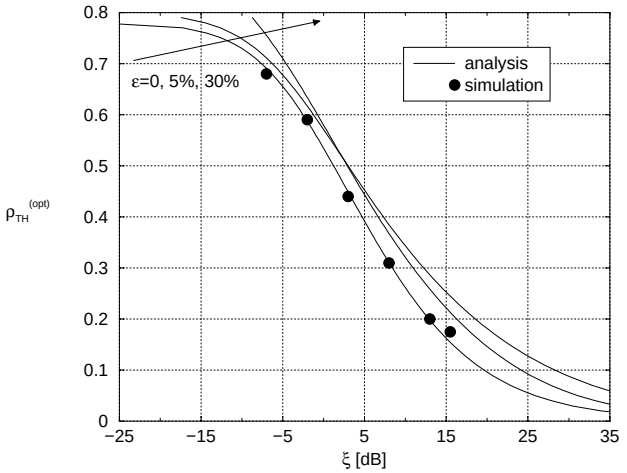

Fig. 5. Optimum ρ_{TH} as a function of ξ: analytical and simulative results. Simulations are for the case of perfect channel estimation.

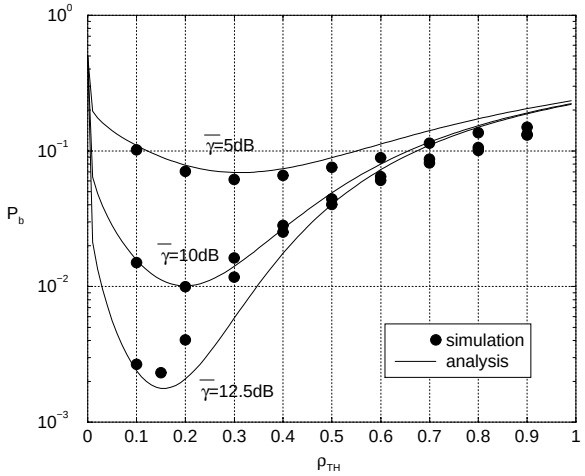

Fig. 6. Analytical and simulated BEP as a function of the threshold ρ_{TH} for different values of mean SNR $\overline{\gamma}$, and $M = N_{\text{u}} = 64$.

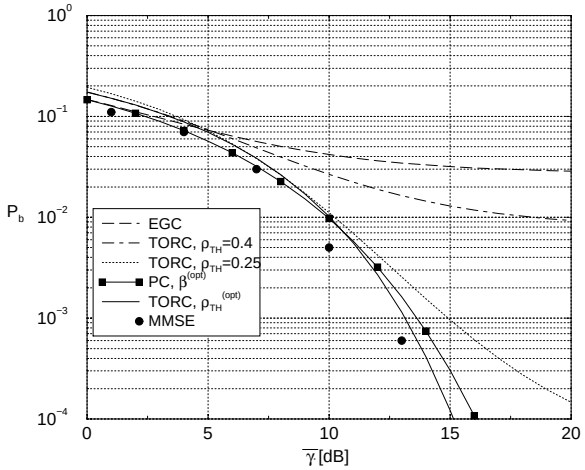

Fig. 7. BEP as a function of the mean SNR $\overline{\gamma}$ in dB for a fully loaded system ($N_{\text{u}} = M = 1024$), when EGC, TORC detector with optimum threshold, TORC with threshold fixed to 0.25 and 0.4, optimum partial combining and MMSE are investigated.

256) system, when varying ε. The strong impact of the choice of ρ_{TH} on the required SNR can be observed; this motivates the fact that, to achieve the target BEP, a suitable value for ρ_{TH} has to be chosen to avoid an unnecessary increasing of $\overline{\gamma}$. Moreover, the low impact of the channel estimation error on the choice of ρ_{TH} with respect to the case of perfect CSI can be appreciated.

From (32) and (36), for the case of ideal and non-ideal CSI, respectively, the evaluation of the optimum value of ρ_{TH} is enabled for different combinations of $\overline{\gamma}$, M, and N_{u}, that is for different values of ξ, as reported in Fig. 5. In particular, the figure states that if the system is noise-limited (low ξ), an optimum TORC detector requires a value for ρ_{TH} close to 1, while, if the system is interference-limited (high ξ), a choice close to ORC (i.e., $\rho_{\text{TH}} = 0$) is required. Monte Carlo simulation results are also provided for the case of perfect CSI, showing a perfect agreement on the optimum ρ_{TH} and, thus, validating our analysis.

B. Ideal Channel Estimation

In Fig. 6 we show the analytical BEP for TORC detection as a function of ρ_{TH} for different values of $\overline{\gamma}$ and $M = N_{\text{u}} = 64$. Simulation results are also given showing the goodness of the presented approach even for a moderate number of subcarriers. Analysis and simulation are in good agreement especially for what concern the value of ρ_{TH} providing the minimum BEP. Moreover, it can be noticed that the choice of the optimum value of ρ_{TH} guarantees a significant performance improvement (which appears more relevant as the mean SNR increases) confirming the literature [11], [12], [14], [18]. Note also that, by increasing the mean SNR, $\overline{\gamma}$, the effect of noise becomes negligible, thus, the optimum value of the threshold minimizing the BEP approaches zero (remember, in fact, that the threshold is chosen to neglect those subchannels contribution highly corrupted by the noise).

In Fig. 7 the performance improvement of an adaptive TORC detector with respect to classical EGC and fixed TORC (with threshold $\rho_{\text{TH}} = 0.25$ and $\rho_{\text{TH}} = 0.4$) is shown for a fully-loaded system ($N_{\text{u}} = M = 1024$) at various SNRs. The BEP for MMSE detection from [23] is also plotted for further comparison. Note that MMSE represents the optimum among the linear combining techniques always providing the better performance and it is less than 1 dB away from what obtained using TORC with the optimum ρ_{TH}. Hence, an adaptive TORC detector allows to obtain performance very close to the optimum but more complex MMSE. For further comparison, the BEP is also plotted for the partial combining (PC) technique presented in [19] with optimum parameter β and it can be observed that TORC outperforms PC as the SNR increases, when the optimal threshold is used.

The case of time and frequency correlated fading channels is considered in Fig. 8, where the simulated BER is plotted as a function of ρ_{TH} when $N_u = M = 64$ for the SUI-1 three-rays channel model [24] (on the three rays: delays 0, 0.4, and 0.9 μs; attenuation 0, 15, and 20 dB referred to omnidirectional antennas; Ricean factor 4, 0, 0; Doppler spectrum 0.4, 0.3, 0.5 Hz, respectively). Different values of

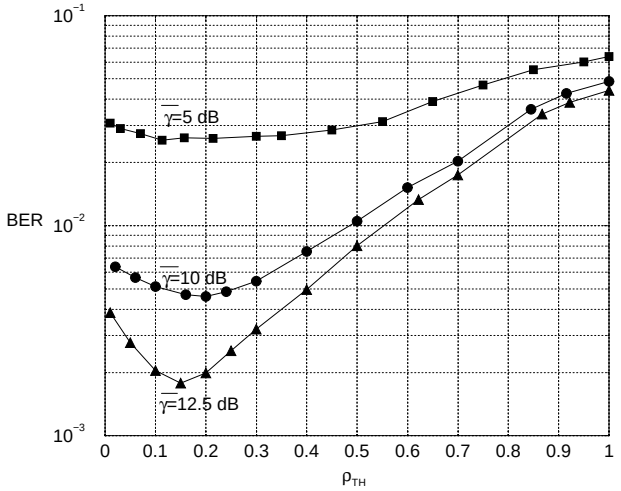

Fig. 8. Simulated BER vs. ρ_{TH} in time and frequency correlated SUI-1 channel varying the mean SNR $\overline{\gamma}$ when $N_u = M = 64$.

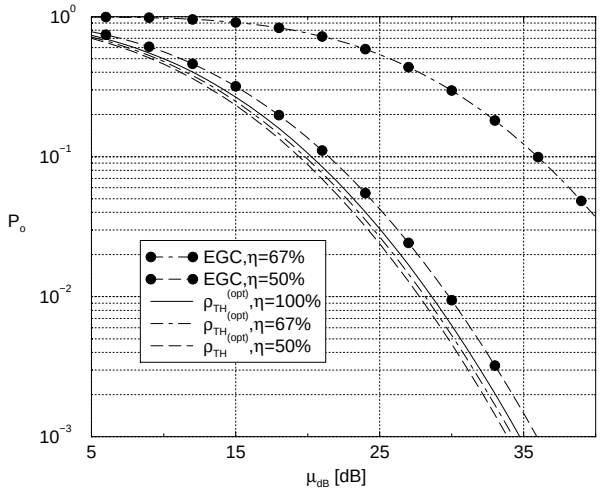

Fig. 9. P_{o} vs. μ_{dB} for $P_{\mathrm{b}}^{\star} = 10^{-2}$, and $\sigma_{\mathrm{dB}} = 8$ varying the system load η: comparison among TORC with optimum use of ρ_{TH} and EGC.

mean SNR, $\overline{\gamma}$, are considered. As can be observed, the BER achieved in this kind of correlated fading channel is inferior to that of uncorrelated fading presented in Fig. 6. Moreover, there is still an optimum value for the threshold giving the minimum BER and this value almost agree with the optimum one in uncorrelated fading. This is an important aspect which highlights how the proposed framework enables to obtain a good value of the TORC threshold also in these kinds of channel.

In Fig. 9, the BEO as a function of the median SNR, μ_{dB}, is reported in uncorrelated fading channel for target BEP $P_{\mathrm{b}}^{\star} = 10^{-2}$ and different system loads when TORC with optimum ρ_{TH} or EGC are adopted in log-normal shadowing with $\sigma_{\mathrm{dB}} = 8$. Fully loaded EGC is not considered since it can not reach the target performance in the considered range for μ_{dB}. In fact $\eta = 67\%$ is the maximum tolerable load which guarantees $P_{\mathrm{b}}^{\star} = 10^{-2}$ with EGC (by adopting MRC, $P_{\mathrm{b}}^{\star} = 10^{-2}$ can be reached with a maximum system load $\eta = 18\%$). It can also be observed that, while the BEO is quite sensitive to the system load for EGC, it is quite insensitive adopting the optimum threshold (i.e., adaptively changing ρ_{TH} to μ_{dB} and η variations).

By fixing both BEP and BEO, our framework enables the derivation of the required median SNR for various system loads. As an example, in Fig. 10, the value of μ_{dB} required by different combining solutions to obtain a target BEP equal to 10^{-2} and a target BEO equal to 1% and 5%, is plotted versus η for $\sigma_{\mathrm{dB}} = 8$. These results show a strong impact of the ρ_{TH} choice on the required μ_{dB}. In particular, when a TORC detector is adopted, the use of the optimum value of ρ_{TH}, following the system load variations, always provides the better performance with respect to a fixed values of ρ_{TH} such as 0.15 or 0.25. The EGC provides the better performance only for low values of η and it is significantly outperformed by adaptive TORC when the system load increases.

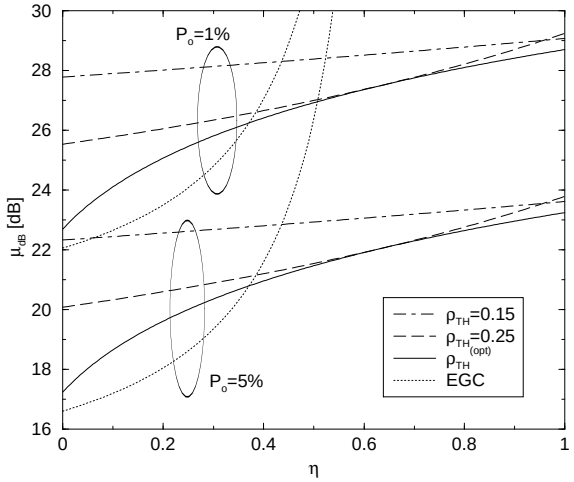

Fig. 10. μ_{dB} vs. η for $P_{\mathrm{b}}^{\star} = 10^{-2}$ and $P_{\mathrm{o}} = 1\%$ and 5%: comparison among TORC with optimum use of ρ_{TH}, TORC with fixed ρ_{TH} equal to 0.15 and 0.25, and EGC.

VIII. Conclusion

In this paper we analyzed the downlink of a MC-CDMA system with TORC detector at the receiver side and evaluated the performance, in terms of both BEP and BEO, with ideal and non-ideal channel estimation. We derived the value of the TORC threshold that optimizes the BEP, showing a non-negligible performance improvement with respect to both the traditional TORC detection with fixed threshold and other linear combining techniques, such as EGC and MRC. We evaluated the optimal threshold as a function of other system parameters, as the number of subcarriers, the number of active users, and the mean SNR averaged over small-scale fading. This opens the way to an adaptive variation of the threshold following slow processes variations. Adaptive TORC significantly improves the performance in fast fading and log-normal shadowing conditions. Moreover, the developed analytical framework allows to assert that the optimum value of the TORC threshold does not significatively change considering

perfect or imperfect CSI, meaning that a system designer can adopt the optimum value of the threshold in perfect CSI conditions also with channel estimation errors. The results are also compared with simulations confirming the validity of the analytical framework. Both uncorrelated and correlated fading channel models have been considered.

APPENDIX
TEST STATISTICS WITH CHANNEL ESTIMATION ERROR

We evaluate the following expressions: (i) $\mathbb{E}\{\Theta(\rho_{\text{TH}})\}$; (ii) $\mathbb{E}\left\{\hat{\alpha}^{-2}u^2(\hat{\alpha}-\rho_{\text{TH}})\right\}$; (iii) $\mathbb{E}\left\{\Theta^2(\rho_{\text{TH}})\right\}$; where $\Theta(\rho_{\text{TH}}) = u(\hat{\alpha}-\rho_{\text{TH}})\alpha\hat{\alpha}^{-1}\cos(\vartheta-\hat{\vartheta})$ and $\hat{\alpha}$ is Rayleigh distributed:

$$p_{\hat{\alpha}}(x) = \frac{x}{\sigma_{\text{h}}^2+\sigma_{\text{e}}^2}e^{-\frac{x^2}{2(\sigma_{\text{h}}^2+\sigma_{\text{e}}^2)}}. \tag{41}$$

The mth estimated complex channel coefficient is $\hat{h}_m = h_m + e_m$. By decomposing in the real and imaginary parts ($h_m = X_m + jY_m$ and $e_m = X_{e_m} + jY_{e_m}$, with j imaginary unit), and since h_m and e_m are zero mean complex Gaussian distributed, then X_m and Y_m, X_{e_m} and Y_{e_m} result zero mean Gaussian distributed with variance σ_{h}^2 and σ_{e}^2, respectively.

For what concern the evaluation of $\mathbb{E}\{\Theta(\rho_{\text{TH}})\}$, it can be written as in (42) at the bottom of this page. By defining now the variables $\tilde{X} = X + X_e$ and $\tilde{Y} = Y + Y_e$, they are the sum of independent zero mean Gaussian RVs, thus distributed as

$$\tilde{X}, \tilde{Y} \sim \mathcal{N}\left(0, \sigma_{\text{h}}^2+\sigma_{\text{e}}^2\right), \tag{43}$$

then, $\mathbb{E}\left\{\tilde{X}\tilde{Y}\right\} = 0$, $\mathbb{E}\left\{\tilde{X}X_e\right\} = \sigma_{\text{e}}^2$ and $\mathbb{E}\left\{\tilde{Y}Y_e\right\} = \sigma_{\text{e}}^2$. Hence, (42) becomes

$$\mathbb{E}\{\Theta(\rho_{\text{TH}})\} = A_1 - A_2,$$

where ($\varepsilon = \sigma_{\text{e}}^2/\sigma_{\text{h}}^2$):

$$A_1 = \mathbb{E}\{u(\hat{\alpha}-\rho_{\text{TH}})\} = \int_{\rho_{\text{TH}}}^{\infty} p_{\hat{\alpha}}(x)dx = e^{-\frac{\rho_{\text{TH}}^2}{2\sigma_{\text{h}}^2(1+\varepsilon)}}. \tag{44}$$

For what concern the term A_2, by passing from cartesian to polar coordinates, thus by defining $r \triangleq \sqrt{\tilde{X}^2+\tilde{Y}^2}$, $\phi' = \text{arctg}(\tilde{Y}/\tilde{X})$, $r_e \triangleq \sqrt{X_e^2+Y_e^2}$ and $\phi_e = \text{arctg}(Y_e/X_e)$, then it can be written as in (45). By considering that

$$\int_0^{2\pi}\int_0^{2\pi}\cos(\phi-\phi_e)e^{\frac{rr_e\cos(\phi-\phi_e)}{2\sigma_{\text{h}}^2}}d\phi d\phi_e = 4\pi^2 I_1\left(\frac{rr_e}{2\sigma_{\text{h}}^2}\right)$$

with $I_1(\cdot)$ being the modified Bessel function of the first kind and order one, then:

$$\begin{aligned}A_2 &= \int_{\rho_{\text{TH}}}^{+\infty} e^{-\frac{r^2}{2\sigma_{\text{h}}^2}}\int_{\rho_{\text{TH}}}^{+\infty} r_e^2\frac{e^{-\left(\frac{1}{2\sigma_{\text{h}}^2}+\frac{1}{2\sigma_{\text{e}}^2}\right)r_e^2}}{\sigma_{\text{e}}^2(\sigma_{\text{h}}^2-\sigma_{\text{e}}^2)}I_1\left(\frac{rr_e}{2\sigma_{\text{h}}^2}\right)dr_e dr\\ &\simeq \int_{\rho_{\text{TH}}}^{+\infty} e^{-\frac{r^2}{2\sigma_{\text{h}}^2}}\left(\frac{\sigma_{\text{e}}^2\sigma_{\text{h}}^2\cdot r\cdot e^{\frac{r^2\sigma_{\text{e}}^2}{8\sigma_{\text{h}}^2(\sigma_{\text{h}}^2+\sigma_{\text{e}}^2)}}}{2(\sigma_{\text{h}}^2-\sigma_{\text{e}}^2)(\sigma_{\text{h}}^2+\sigma_{\text{e}}^2)^2}\right)dr\\ &= \frac{4\sigma_{\text{h}}^4\sigma_{\text{e}}^2 e^{-\frac{\rho_{\text{TH}}^2(4\sigma_{\text{h}}^2+3\sigma_{\text{e}}^2)}{8\sigma_{\text{h}}^2(\sigma_{\text{h}}^2+\sigma_{\text{e}}^2)}}}{2(\sigma_{\text{h}}^2-\sigma_{\text{e}}^2)(\sigma_{\text{h}}^2+\sigma_{\text{e}}^2)(4\sigma_{\text{h}}^2+3\sigma_{\text{e}}^2)}.\end{aligned}$$

Finally we can write:

$$\mathbb{E}\{\Theta(\rho_{\text{TH}})\} = e^{-\frac{\rho_{\text{TH}}^2}{2\sigma_{\text{h}}^2(1+\varepsilon)}} - \frac{2\varepsilon e^{-\frac{\rho_{\text{TH}}^2(4+3\varepsilon)}{8\sigma_{\text{h}}^2(1+\varepsilon)}}}{(1-\varepsilon^2)(4+3\varepsilon)}. \tag{46}$$

For what concern the second term to be evaluated:

$$\begin{aligned}\mathbb{E}\left\{\hat{\alpha}^{-2}u^2(\hat{\alpha}-\rho_{\text{TH}})\right\} &= \frac{1}{2(\sigma_{\text{h}}^2+\sigma_{\text{e}}^2)}\Gamma\left[0, \frac{\rho_{\text{TH}}^2}{2(\sigma_{\text{h}}^2+\sigma_{\text{e}}^2)}\right]\\ &= \frac{1}{2\sigma_{\text{h}}^2(1+\varepsilon)}\Gamma\left[0, \frac{\rho_{\text{TH}}^2}{2\sigma_{\text{h}}^2(1+\varepsilon)}\right],\end{aligned} \tag{47}$$

being $\Gamma[0,x]$ the incomplete Euler Gamma function.

The term $\mathbb{E}\left\{\Theta^2(\rho_{\text{TH}})\right\}$ is given in (48), where $A_3 = A_1$, whereas A_4 and A_5 are evaluated in the following. By chang-

$$\begin{aligned}\mathbb{E}\{\Theta(\rho_{\text{TH}})\} &= \mathbb{E}\left\{u(\hat{\alpha}-\rho_{\text{TH}})\alpha\hat{\alpha}^{-1}\cos(\vartheta-\hat{\vartheta})\right\} = \mathbb{E}\left\{u(\hat{\alpha}-\rho_{\text{TH}})\alpha\hat{\alpha}^{-1}(\cos\vartheta\cos\hat{\vartheta}+\sin\vartheta\sin\hat{\vartheta})\right\}\\ &= \mathbb{E}\left\{u(\hat{\alpha}-\rho_{\text{TH}})\sqrt{X^2+Y^2}\left(\sqrt{(X+X_e)^2+(Y+Y_e)^2}\right)^{-1}\frac{X(X+X_e)+Y(Y+Y_e)}{\sqrt{X^2+Y^2}\sqrt{(X+X_e)^2+(Y+Y_e)^2}}\right\}\\ &= \mathbb{E}\left\{u(\hat{\alpha}-\rho_{\text{TH}})[(X+X_e)^2+(Y+Y_e)^2]^{-1}[X(X+X_e)+Y(Y+Y_e)]\right\}.\end{aligned} \tag{42}$$

$$\begin{aligned}A_2 &= \mathbb{E}\left\{u(\hat{\alpha}-\rho_{\text{TH}})(\tilde{X}^2+\tilde{Y}^2)^{-1}(\tilde{X}X_e+\tilde{Y}Y_e)\right\} = \int_{\rho_{\text{TH}}}^{+\infty}\int_{\rho_{\text{TH}}}^{+\infty}\int_{\rho_{\text{TH}}}^{+\infty}\int_{\rho_{\text{TH}}}^{+\infty}(\tilde{X}^2+\tilde{Y}^2)^{-1}(\tilde{X}X_e+\tilde{Y}Y_e)\\ &\quad\times\frac{e^{-\frac{1}{2}[\frac{1}{\sigma_{\text{h}}^2}(\tilde{X}^2+\tilde{Y}^2)-\frac{1}{\sigma_{\text{h}}^2}(\tilde{X}Y_e+\tilde{Y}X_e)+(\frac{1}{\sigma_{\text{h}}^2}+\frac{1}{\sigma_{\text{e}}^2})(X_e^2+Y_e^2)]}}{4\pi^2\sigma_{\text{e}}^2(\sigma_{\text{h}}^2-\sigma_{\text{e}}^2)}d\tilde{X}dX_e d\tilde{Y}dY_e\\ &= \int_{\rho_{\text{TH}}}^{+\infty}\int_{\rho_{\text{TH}}}^{+\infty}\int_0^{2\pi}\int_0^{2\pi}r^{-2}rr_e\cos(\phi-\phi_e)\frac{e^{-\left[\frac{r^2}{2\sigma_{\text{h}}^2}+\left(\frac{1}{2\sigma_{\text{h}}^2}+\frac{1}{2\sigma_{\text{e}}^2}\right)r_e^2\right]}}{4\pi^2\sigma_{\text{e}}^2(\sigma_{\text{h}}^2-\sigma_{\text{e}}^2)}e^{\frac{rr_e\cos(\phi-\phi_e)}{2\sigma_{\text{h}}^2}}rr_e dr dr_e d\phi d\phi_e\\ &= \int_{\rho_{\text{TH}}}^{+\infty}\int_{\rho_{\text{TH}}}^{+\infty}r_e^2\frac{e^{-\left[\frac{r^2}{2\sigma_{\text{h}}^2}+\left(\frac{1}{2\sigma_{\text{h}}^2}+\frac{1}{2\sigma_{\text{e}}^2}\right)r_e^2\right]}}{4\pi^2\sigma_{\text{e}}^2(\sigma_{\text{h}}^2-\sigma_{\text{e}}^2)}\left(\int_0^{2\pi}\int_0^{2\pi}\cos(\phi-\phi_e)e^{\frac{rr_e\cos(\phi-\phi_e)}{2\sigma_{\text{h}}^2}}d\phi d\phi_e\right)dr dr_e.\end{aligned} \tag{45}$$

ing coordinates into polars, we can write

$$A_4 = \int_{\rho_{\text{TH}}}^{+\infty} r^{-1} e^{-\frac{r^2}{2\sigma_{\text{h}}^2}} \times \underbrace{\left(\int_{\rho_{\text{TH}}}^{+\infty} r_e^3 \frac{e^{-\left(\frac{1}{2\sigma_{\text{h}}^2}+\frac{1}{2\sigma_{\text{e}}^2}\right) r_e^2}}{\sigma_{\text{e}}^2(\sigma_{\text{h}}^2 - 2\sigma_{\text{e}}^2)} I_1\left(\frac{r r_e}{2\sigma_{\text{h}}^2}\right) dr_e \right)}_{A_4'} dr \,, \tag{49}$$

where

$$A_4' \simeq \frac{\sqrt{\pi}\sigma_{\text{e}}^2 r e^{\frac{\sigma_{\text{e}}^2 r^2}{16\sigma_{\text{h}}^2(\sigma_{\text{h}}^2+\sigma_{\text{e}}^2)}}}{4\sqrt{\frac{1}{2\sigma_{\text{h}}^2}+\frac{1}{2\sigma_{\text{e}}^2}}(2\sigma_{\text{h}}^2+2\sigma_{\text{e}}^2)^3} \times \left\{ \frac{12\sigma_{\text{h}}^4 + 12\sigma_{\text{h}}^2\sigma_{\text{e}}^2 + \sigma_{\text{e}}^2 r^2}{\sigma_{\text{h}}^2 - \sigma_{\text{e}}^2} \cdot I_0\left[\frac{\sigma_{\text{e}}^2 r^2}{16\sigma_{\text{h}}^2(\sigma_{\text{h}}^2+\sigma_{\text{e}}^2)}\right] + \frac{4\sigma_{\text{h}}^2 + 4\sigma_{\text{h}}^2\sigma_{\text{e}}^2 + \sigma_{\text{e}}^2 r^2}{\sigma_{\text{h}}^2 - \sigma_{\text{e}}^2} \cdot I_1\left[\frac{\sigma_{\text{e}}^2 r^2}{16\sigma_{\text{h}}^2(\sigma_{\text{h}}^2+\sigma_{\text{e}}^2)}\right] \right\}.$$

Then A_4 results in (50), with

$$C = \frac{\sqrt{\pi}\cdot\varepsilon}{\sqrt{\frac{1+\varepsilon}{2\sigma_{\text{e}}^2}} 4\sigma_{\text{h}}^4(1-\varepsilon)(1+\varepsilon)^2}$$

$$B_1 \simeq \frac{3\sigma_{\text{h}}^3}{2}\sqrt{\frac{2}{\pi}} K\left(\frac{\varepsilon}{4(1+\varepsilon)}\right) = 3\sigma_{\text{h}}^2\sqrt{\pi}\left(\frac{8+7\varepsilon}{\sigma_{\text{h}}^2(1+\varepsilon)}\right)^{-1/2} {}_2F_1\left[\frac{1}{4},\frac{3}{4},1,\frac{\varepsilon^2}{(8+7\varepsilon)^2}\right]$$

$$B_2 \simeq \frac{\varepsilon}{(1+\varepsilon)} \frac{2\sqrt{\pi}\ {}_2F_1\left[\frac{3}{4},\frac{5}{4},1,\frac{\varepsilon^2}{(8+7\varepsilon)^2}\right]}{\left(\frac{8+7\varepsilon}{\sigma_{\text{h}}^2(1+\varepsilon)}\right)^{3/2}}$$

$$B_3 \simeq \frac{\sqrt{\pi}\sigma_{\text{e}}^2\sigma_{\text{h}}}{4(8+7\varepsilon)}\sqrt{\frac{1+\varepsilon}{8+7\varepsilon}}\ {}_2F_1\left[\frac{3}{4},\frac{5}{4},2,\frac{\varepsilon^2}{(8+7\varepsilon)^2}\right]$$

$$B_4 \simeq \frac{3\sqrt{\pi}\varepsilon^2}{2(1+\varepsilon)} \frac{{}_2F_1\left[\frac{5}{4},\frac{7}{4},2,\frac{\varepsilon^2}{(8+7\varepsilon)^2}\right]}{(8+7\varepsilon)\left(\frac{8+7\varepsilon}{\sigma_{\text{h}}^2(1+\varepsilon)}\right)^{3/2}},$$

being I_0 the modified Bessel function of the first kind and order zero, $K(m)$ the complete elliptic integral of the first kind, and ${}_2F_1[a,b,c,z]$ the hypergeometric function.

By following the same procedure applied to A_4 also for the term A_5, we obtain

$$\begin{aligned} A_5 &= \int_{\rho_{\text{TH}}}^{+\infty} e^{-\frac{r^2}{2\sigma_{\text{h}}^2}} \int_{\rho_{\text{TH}}}^{+\infty} r_e^2 \frac{e^{-\left(\frac{1}{2\sigma_{\text{h}}^2}+\frac{1}{2\sigma_{\text{e}}^2}\right) r_e^2}}{\sigma_{\text{e}}^2(\sigma_{\text{h}}^2-\sigma_{\text{e}}^2)} I_1\left(\frac{r r_e}{2\sigma_{\text{h}}^2}\right) dr_e dr \\ &\simeq \int_{\rho_{\text{TH}}}^{+\infty} e^{-\frac{r^2}{2\sigma_{\text{h}}^2}} \left(\frac{\sigma_{\text{e}}^2\sigma_{\text{h}}^2 \cdot r \cdot e^{\frac{r^2\sigma_{\text{e}}^2}{8\sigma_{\text{h}}^2(\sigma_{\text{h}}^2+\sigma_{\text{e}}^2)}}}{2(\sigma_{\text{h}}^2-\sigma_{\text{e}}^2)(\sigma_{\text{h}}^2+\sigma_{\text{e}}^2)^2} \right) dr \\ &= \frac{2\sigma_{\text{h}}^4\sigma_{\text{e}}^2}{(\sigma_{\text{h}}^2-\sigma_{\text{e}}^2)(\sigma_{\text{h}}^2+\sigma_{\text{e}}^2)(4\sigma_{\text{h}}^2+3\sigma_{\text{e}}^2)} e^{-\frac{\rho_{\text{TH}}^2}{8}\left(\frac{3}{\sigma_{\text{h}}^2}+\frac{1}{\sigma_{\text{h}}^2+\sigma_{\text{e}}^2}\right)} \\ &= \frac{2\varepsilon}{(1-\varepsilon^2)(4+3\varepsilon)} e^{-\frac{\rho_{\text{TH}}^2}{8}\left(\frac{4+3\varepsilon}{\sigma_{\text{h}}^2(1+\varepsilon)}\right)}. \end{aligned} \tag{51}$$

Hence,

$$\mathbb{E}\left\{\Theta^2(\rho_{\text{TH}})\right\} \simeq A_3 + A_4 - 2A_5\,. \tag{52}$$

$$\begin{aligned} &\mathbb{E}\left\{\Theta_l^2(\rho_{\text{TH}})\right\} = \mathbb{E}\left\{u^2(\hat{\alpha}-\rho_{\text{TH}})\alpha_l^2\hat{\alpha}_l{}^{-2}\cos^2(\theta_l-\hat{\theta}_l)\right\} = \mathbb{E}\left\{u^2(\hat{\alpha}-\rho_{\text{TH}})(\tilde{X}^2+\tilde{Y}^2)^{-2}[(\tilde{X}^2+\tilde{Y}^2)-(\tilde{X}X_e+\tilde{Y}Y_e)]^2\right\} \\ &= \mathbb{E}\left\{u^2(\hat{\alpha}-\rho_{\text{TH}})(\tilde{X}^2+\tilde{Y}^2)^{-2}[(\tilde{X}^2+\tilde{Y}^2)^2+(\tilde{X}X_e+\tilde{Y}Y_e)^2-2(\tilde{X}^2+\tilde{Y}^2)(\tilde{X}X_e+\tilde{Y}Y_e)]\right\} \\ &= \underbrace{\mathbb{E}\left\{u^2(\hat{\alpha}-\rho_{\text{TH}})\right\}}_{A_3} + \underbrace{\mathbb{E}\left\{u^2(\hat{\alpha}-\rho_{\text{TH}})(\tilde{X}^2+\tilde{Y}^2)^{-2}(\tilde{X}X_e+\tilde{Y}Y_e)^2\right\}}_{A_4} - 2\underbrace{\mathbb{E}\left\{u^2(\hat{\alpha}-\rho_{\text{TH}})(\tilde{X}^2+\tilde{Y}^2)^{-1}(\tilde{X}X_e+\tilde{Y}Y_e)\right\}}_{A_5}, \end{aligned} \tag{48}$$

$$\begin{aligned} A_4 &\simeq \overbrace{\frac{\sqrt{\pi}\sigma_{\text{e}}^2}{\sqrt{\frac{1}{2\sigma_{\text{h}}^2}+\frac{1}{2\sigma_{\text{e}}^2}}(2\sigma_{\text{h}}^2+2\sigma_{\text{e}}^2)^2(\sigma_{\text{h}}^2-\sigma_{\text{e}}^2)}}^{C} \int_{\rho_{\text{TH}}}^{+\infty} e^{-\frac{r^2}{2\sigma_{\text{h}}^2}\left(1-\frac{\sigma_{\text{e}}^2}{8(\sigma_{\text{h}}^2+\sigma_{\text{e}}^2)}\right)} \\ &\times \left\{ \left(\frac{3}{2}\sigma_{\text{h}}^2 + \frac{\sigma_{\text{e}}^2 r^2}{8(\sigma_{\text{h}}^2+\sigma_{\text{e}}^2)}\right) I_0\left[\frac{\sigma_{\text{e}}^2 r^2}{16\sigma_{\text{h}}^2(\sigma_{\text{h}}^2+\sigma_{\text{e}}^2)}\right] + \left(\frac{1}{2}\sigma_{\text{h}}^2 + \frac{\sigma_{\text{e}}^2 r^2}{8(\sigma_{\text{h}}^2+\sigma_{\text{e}}^2)}\right) I_1\left[\frac{\sigma_{\text{e}}^2 r^2}{16\sigma_{\text{h}}^2(\sigma_{\text{h}}^2+\sigma_{\text{e}}^2)}\right] \right\} dr \\ &= C \cdot \left\{ \overbrace{\int_{\rho_{\text{TH}}}^{+\infty} \frac{3}{2}\sigma_{\text{h}}^2 e^{-\frac{r^2}{2\sigma_{\text{h}}^2}\left(1-\frac{\sigma_{\text{e}}^2}{8(\sigma_{\text{h}}^2+\sigma_{\text{e}}^2)}\right)} I_0\left[\frac{\sigma_{\text{e}}^2 r^2}{16\sigma_{\text{h}}^2(\sigma_{\text{h}}^2+\sigma_{\text{e}}^2)}\right] dr}^{B_1} + \overbrace{\int_{\rho_{\text{TH}}}^{+\infty} \frac{\sigma_{\text{e}}^2 r^2}{8(\sigma_{\text{h}}^2+\sigma_{\text{e}}^2)} e^{-\frac{r^2}{2\sigma_{\text{h}}^2}\left(1-\frac{\sigma_{\text{e}}^2}{8(\sigma_{\text{h}}^2+\sigma_{\text{e}}^2)}\right)} I_0\left[\frac{\sigma_{\text{e}}^2 r^2}{16\sigma_{\text{h}}^2(\sigma_{\text{h}}^2+\sigma_{\text{e}}^2)}\right] dr}^{B_2} \right. \\ &\left. + \overbrace{\int_{\rho_{\text{TH}}}^{+\infty} \frac{1}{2}\sigma_{\text{h}}^2 e^{-\frac{r^2}{2\sigma_{\text{h}}^2}\left(1-\frac{\sigma_{\text{e}}^2}{8(\sigma_{\text{h}}^2+\sigma_{\text{e}}^2)}\right)} I_1\left[\frac{\sigma_{\text{e}}^2 r^2}{16\sigma_{\text{h}}^2(\sigma_{\text{h}}^2+\sigma_{\text{e}}^2)}\right] dr}^{B_3} + \overbrace{\int_{\rho_{\text{TH}}}^{+\infty} \frac{\sigma_{\text{e}}^2 r^2}{8(\sigma_{\text{h}}^2+\sigma_{\text{e}}^2)} e^{-\frac{r^2}{2\sigma_{\text{h}}^2}\left(1-\frac{\sigma_{\text{e}}^2}{8(\sigma_{\text{h}}^2+\sigma_{\text{e}}^2)}\right)} I_1\left[\frac{\sigma_{\text{e}}^2 r^2}{16\sigma_{\text{h}}^2(\sigma_{\text{h}}^2+\sigma_{\text{e}}^2)}\right] dr}^{B_4} \right\} \end{aligned} \tag{50}$$

ACKNOWLEDGMENTS

The authors would like to acknowledge Prof. O. Andrisano for motivating and supporting this research activity, Proff. M. Chiani and M.Z. Win for helpful comments on adaptive techniques, and F. Zabini for helpful discussions on equalization techniques for MC-CDMA systems.

REFERENCES

[1] K. Fazel and S. Kaiser, "Multi-Carrier and Spread Spectrum Systems". New York: Wiley, 2003.

[2] N. Yee, J.-P. Linnartz and G. Fettweis, "Multi-Carrier-CDMA in indoor wireless networks", in Conference Proceedings PIMRC '93, Yokohama, Sept, 1993. p 109-113.

[3] S. Hara and R. Prasad, "An Overview of multicarrier CDMA", IEEE 4th International Symposium on Spread Spectrum Techniques and Applications Proceedings, 22-25 Sept. 1996, Pages:107 - 114 vol.1.

[4] N. Yee and J.-P. Linnartz, "BER of multi-carrier CDMA in an indoor Rician fading channel", Conference Record of The Twenty-Seventh Asilomar Conference on Signals, Systems and Computers, 1993., 1-3 Nov. 1993 Pages:426 - 430 vol.1.

[5] S. Kaiser, "On the performance of different detection techniques for OFDM-CDMA in fading channels", in *Globecom '95 pp.2059-2063 Nov. 1995*

[6] L. Sanguinetti, I. Cosovic, M. Morelli, "Channel estimation for MC-CDMA uplink transmissions with combined equalization", Selected Areas in Communications, IEEE Journal on Volume 24, Issue 6, June 2006 Page(s):1167 - 1178.

[7] I. Cosovic, M. Schnell, A. Springer, "Combined equalization for uplink MC-CDMA in Rayleigh fading channels", Communications, IEEE Transactions on Volume 53, Issue 10, Oct. 2005 Page(s):1609 - 1614.

[8] M. K. Simon and M. S. Alouini, "Digital Communication over Fading Channels", New York, NY, 10158: John Wiley & Sons, Inc., second ed., 2004.

[9] M. Z. Win and J. H. Winters, "Virtual branch analysis of symbol error probability for hybrid selection/maximal-ratio combining in Rayleigh fading", IEEE Trans. Commun., vol. 49, pp. 19261934, Nov. 2001.

[10] M. Z. Win, G. Chrisikos, and J. H. Winters, "MRC performance for M-ary modulation in arbitrarily correlated Nakagami fading channels", IEEE Commun. Lett., vol. 4, pp. 301303, Oct. 2000.

[11] Kalofonos, D.N.; Stojanovic, M.; Proakis, J.G., "Performance of adaptive MC-CDMA detectors in rapidly fading Rayleigh channels", Wireless Communications, IEEE Transactions on Volume 2, Issue 2, March 2003 Page(s):229 - 239.

[12] T. Müller, H. Rohling and R. Grünheid, "Comparison of different Detection Algorithms for OFDM-CDMA in Broadband Rayleigh Fading",Vehicular Technology Conference, 1995 IEEE 45th Volume 2, 25-28 July 1995 Page(s):835 - 838.

[13] N. Yee and J.-P. Linnartz, "Controlled equalization of multi-carrier CDMA in an indoor Rician fading channel" in *Vehicular Technology Conference, 1994 IEEE 44th ,8-10 June 1994 Pages:1665 - 1669 vol.3.*

[14] Kalofonos, D.N.; Proakis, J.G., "Performance of the multi-stage detector for a MC-CDMA system in a Rayleigh fading channel", Global Telecommunications Conference, 1996. GLOBECOM '96. 'Communications: The Key to Global Prosperity Volume 3, 18-22 Nov. 1996 Page(s):1784 - 1788.

[15] A. Conti, M. Win, M. Chiani, J.H. Winters "Bit Error Outage for Diversity Reception in Shadowing Environment", IEEE Communications Letters, Volume: 07 , Issue: 1 , Jan. 2003. Pages: 15 - 17.

[16] A. Conti, M. Win, M. Chiani, "Slow Adaptive M-QAM with Diversity inFast Fading and Shadowing", IEEE Transactions on Communications, Vol. 55, Issue 5, May 2007, Page(s): 895-905.

[17] O. Andrisano, V. Tralli, R. Verdone, "Millimeter waves for short-range multimedia communication systems", Proceedings of the IEEE, Volume: 86, Issue: 7, July 1998, pp. 1383-1401.

[18] I. Cosovic, S. Kaiser, "A Unified Analysis of Diversity Exploitation in Multicarrier CDMA", IEEE Transactions on Vehicular Technology, Vol. 56, No 4, Pages: 2051 - 2062, July 2007.

[19] A. Conti, B. M. Masini, F. Zabini and O. Andrisano, "On the downlink Performance of Multi-Carrier CDMA Systems with Partial Equalization", IEEE Transactions on Wireless Communications, Volume 6, Issue 1, Jan. 2007, Page(s):230 - 239.

[20] W.M. Gifford, M.Z. Win, M. Chiani "Antenna subset diversity with non-ideal channel estimation", Wireless Communications, IEEE Transactions on Volume 7, Issue 5, Part 1, May 2008 Page(s):1527 - 1539.

[21] V. Erceg, L. J. Greenstein, S. Y. Tjandra, S. R. Parkoff, A. Gupta, B. Kulic, A. A. Julius, R. Bianchi, "An empirically based path loss model for wireless channels in suburban environments", Selected Areas in Communications, IEEE Journal on Volume 17, Issue 7, July 1999 Page(s):1205 - 1211.

[22] A. Conti, M. Z. Win, M. Chiani, "On the inverse symbol-error probability for diversity reception", Communications, IEEE Transactions on, Volume: 51, Issue: 5, page(s): 753- 756, May 2003.

[23] S.B. Slimane, "Partial equalization of multi-carrier CDMA in frequency selective fading channels", IEEE International Conference on Communications, 2000, Volume: 1 ,18-22 June 2000 Pages:26 - 30.

[24] V. Erceg, K.V.S. Hari, M.S. Smith, D.S. Baum et al, "Channel Models for Fixed Wireless Applications", revised version of the document IEEE 802.16.3c-01/29r4. The IEEE 802.16 Working Group on Broadband Wireless Access Standards. http://wirelessman.org/tga/docs/80216a-03_01.pdf

Barbara M. Masini (S'02-M'05) received the Laurea degree (with honors) and the Ph.D. degree in telecommunications engineering from the University of Bologna, Italy, in 2001 and 2005, respectively. In 2002, she joined the Department of Electronics, Informatics and Systems at the University of Bologna, to develop his research activity in the area of wireless communications. Since 2005, she is with the Institute for Electronics and for Information and Telecommunications Engineering (IEIIT), Research Unit of Bologna, of the National Research Council (CNR) working on wireless transmission techniques. Since 2007 she is assistant professor at the University of Bologna where she holds the course of Telecommunication Laboratory including experimental implementation of telecommunication systems on digital signal processing platforms.

Her research interests are mainly focused on OFDM and MC-CDMA systems, short-range wireless communications, wireless local-area networks (WLAN), and coexistence among different wireless systems. She is also interested in intelligent transportation systems (ITS) for infomobility applications and is coauthor of the chapter *Heterogeneous wireless communications for vehicular network* in the book *Vehicular Networks: Techniques, Standards, and Applications*, CRC Press, 2009.

She is an IEEE member, and serves as a Reviewer for many Transactions and Conferences and as a TPC Member for several Conferences.

Andrea Conti (S'99-M'01) received the Dr.Ing. degree in telecommunications engineering and the Ph.D. degree in electronic engineering and computer science from the University of Bologna, Italy, in 1997 and 2001, respectively. Since 2005, he is assistant professor at the University of Ferrara, Italy. Prior to joining the University of Ferrara he was with Consorzio Nazionale Interuniversitario per le Telecomunicazioni (CNIT, 1999-2002) and Istituto di Elettronica e di Ingegneria dell'Informazione e delle Telecomunicazioni, Consiglio Nazionale delle Ricerche (IEIIT/CNR, 2002-2005) at the Research Unit of Bologna, Italy. In summer 2001, he joined the Wireless Section of AT&T Research Laboratories, Middletown, NJ. Since February 2003, he has been a frequent visitor at the Laboratory for Information and Decision Systems (LIDS), Massachusetts Institute of Technology (MIT), Cambridge, where he is presently research affiliate.

His current research interests are in the area of wireless communications including localization, adaptive transmission and multichannel reception, coding in faded multiple-input multiple-output channels, wireless cooperative networks, and wireless sensor networks.

He is a coauthor of "Wireless Sensor and Actuator Networks: Enabling Technologies, Information Processing and Protocol Design" (Elsevier, 2008). He is an Editor for the IEEE TRANSACTIONS ON WIRELESS COMMUNICATIONS and was Lead Editor for the EURASIP JASP (S.I. on Wireless Cooperative Networks, 2008). He is TPC Vice-Chair for IEEE WCNC 2009, Co-Chair of the Wireless Comm. Symp. for IEEE GCC 2010, and has served as a Reviewer and TPC member for various IEEE journals and conferences. He is currently serving as secretary of IEEE RCC for the period 2008-2010.